Design optimization of Aalborg-type transformer-less PV inverters with focus on power quality

Georgios I. Orfanoudakis
HELLENIC MEDITERRANEAN UNIVERSITY (HMU), GREECE
Department of Electrical Engineering
Estauromenos, 71004
Heraklion, Crete, Greece
E-mail: gorfas@hmu.gr

Georgios Foteinopoulos
TECHNICAL UNIVERSITY OF CRETE (TUC), GREECE
School of Electrical & Computer Engineering,
University Campus, 73100
Chania, Crete, Greece
E-mail: georgefwt@gmail.com

Eftychios Koutroulis
TECHNICAL UNIVERSITY OF CRETE (TUC), GREECE
School of Electrical & Computer Engineering,
University Campus, 73100
Chania, Crete, Greece
E-mail: efkout@electronics.tuc.gr

Weimin Wu
SHANGHAI MARITIME UNIVERSITY, CHINA
Department of Electrical Engineering,
Shanghai, 201306, China
E-mail: wmwu@shmtu.edu.cn

***Abstract*—Single-phase transformerless photovoltaic (PV) inverters are based on unconventional power circuit topologies and are required to achieve very high efficiency and power quality over their entire operating range. Optimization techniques applied to conventional converter topologies need to be extended to cover these requirements. This paper proposes a PV inverter design optimization method for Aalborg-type transformerless PV inverters which integrates simulations in an optimization algorithm to maximize the inverter European efficiency, while abiding by the power quality limits set by relevant standards. According to it, the entire PV system, including the PV array, the PV inverter with its controller, and the grid are simulated in MATLAB-Simulink to estimate the inverter losses and output current distortion for design alternatives devised by the optimization algorithm. Design results obtained on an Aalborg-type transformerless PV inverter, indicate that its European efficiency can be maximized under different sets of constraints, while maintaining permissible output current quality at all power levels.**

Keywords—Photovoltaic (PV) inverter, Transformerless inverter, Optimization, Particle Swarm Optimization (PSO)

I. INTRODUCTION

Transformerless photovoltaic (PV) inverters have dominated the single-phase PV inverter market during the last two decades. Obtaining a high efficiency and power quality has been a primary target for all proposed transformerless topologies. In order to achieve this target, main design parameters such as the switching frequency and filter inductance and capacitance values must be optimized.

Optimization algorithms, mainly based on metaheuristic methods [1, 2], have been applied for the design of several types of power converters, such as DC-DC converters used in power supplies and inverters for motor drive applications [1 – 9]. The performance metrics employed as objective functions of the optimization process are typically the efficiency, volume (power density), mass, cost and reliability of the converter. The power quality requirements are normally considered in an approximate manner, through fundamental mathematical models relating for example the converter switching frequency with the cut-off frequency or ripple factor of its filters [10, 11].

Moreover, in several applications, the optimization aims to maximize the inverter efficiency for a given load, at which it is known that it will normally operate. With reference to PV inverters, however, the load profile varies widely, ranging from very low to nominal power, due to the daily and seasonal variations of solar irradiance and ambient temperature. Both the inverter efficiency and output current quality are affected by the load variation. Furthermore, the output current quality requirements are specified in detail in standards for distributed generation [12] and harmonic control [13], which set limits for the grid current total demand distortion (TDD) and for the amplitudes of its individual harmonics. Different methods have been proposed in the literature for the design of filters for grid-connected inverters that can help meet the above requirements [14]. However, these methods are only applicable to conventional, i.e. voltage-source, inverters and not for topologies with current-source characteristics.

Circuit simulators have also been employed in the past to support the task of optimizing power converters [15 – 20]. However, they were not always used in conjunction with optimization algorithms, while they were primarily applied for the estimation of converter losses and to confirm the fulfilling of fundamental constraints.

This paper proposes the integration of a powerful simulator into an optimization algorithm, with the aim of maximizing the European efficiency [10] of a modern transformerless PV inverter topology. The topology exhibits both voltage- and current-source characteristics, thus filter design methods and control techniques for conventional grid-connected inverters are not applicable to it. The simulation model includes the PV array, the inverter with its controller, and the grid, which allows it to derive the expected grid current TDD and the individual component losses, at different power levels. The proposed design optimization algorithm appropriately selects the values of critical design parameters and rejects combinations resulting in high current TDD, so that it limits the number of executed simulations. The design parameter values resulting from the European efficiency optimization procedure therefore also provide acceptable current TDD for the entire range of inverter operation.

II. Background

A. Aalborg PV inverter topology

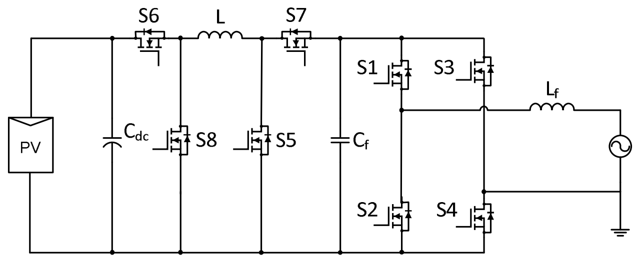

Fig. 1. Full-bridge Aalborg inverter with synchronous Buck/Boost stages.

The PV inverter used as a test bed for applying the proposed optimization method is an improved version of the Full-bridge Aalborg transformerless PV inverter [21], shown in Fig. 1. This inverter possesses PV array voltage step-up capability and includes three different power stages: a synchronous Buck (S6 – S8), a synchronous Boost (S5 – S7) and a DC/AC stage (S1 – S4). It belongs to the family of “Buck in Buck, Boost in Boost” PV inverters, which denotes that only one power stage, namely the Buck or the Boost stage, switches at high frequency at each moment. This provides the basis for achieving high efficiencies, in the order of 97 – 98% [21].

The topology operates in Buck mode for the periods when the peak output voltage is lower than the PV array voltage, while it operates in Boost mode when the peak output voltage exceeds the PV array voltage. Due to its Buck/Boost characteristics, the inverter requires a custom current control technique to operate as a grid-connected inverter. For the purposes of the present study, the inverter is controlled according to the approach described in [22].

B. Particle Swarm Optimization

The proposed optimization method employs the Particle Swarm Optimization (PSO) algorithm, first presented in [23]. The PSO is an optimization algorithm that utilizes a number of particles that move around the search space of a problem. Each particle evaluates the outcome of this problem, i.e. the objective function, at its current position, that is, with a certain value for each of the design variables. The major advantage of the PSO algorithm comes from the way the particles interact with each other. After each iteration of the algorithm, each particle moves to a new position. This position results from a formula that combines the particle’s previous position and best outcome up to this point, as well as the best positions of some of its neighbors. It can be shown that after a given number of iterations, the PSO algorithm identifies values for the design variables that closely approximate the global minimum/maximum of the objective function.

III. Proposed Optimization Method

A. Critical design parameters

According to the proposed optimization method, the PSO algorithm is employed to estimate the optimal values for critical design parameters of the PV inverter. These are the Buck/Boost stage switching frequency, the Buck/Boost inductor (L), the output filter inductor (L_f) and the Buck/Boost output capacitor (C). The minimum/maximum allowed values for these parameters are listed in Table I.

TABLE I. Design Parameters and Their Boundary Values

Symbol	Description	Min / Max	Unit
f_s	Buck/Boost switching freq.	10 / 20	kHz
L	Buck/Boost inductor	0.5 / 2.5	mH
L_f	Output filter inductor	0.02 / 1.5	mH
C	Buck/Boost output capacitor	2 / 5	μF

B. Link of PSO with MATLAB-Simulink

The objective function of the PSO algorithm (1) is the European efficiency, η_{eu}, of the PV inverter (2), which must be maximized under the constraint of maintaining an output current TDD below 5% [12] under all power conditions.

$$\underset{\substack{\boldsymbol{X}=[f_{sw},L,L_f,C] \\ TDD<5\%}}{\text{maximize}}\ \eta_{eu}(\boldsymbol{X}) \tag{1}$$

where:

$$\eta_{eu} = 0.03 \cdot \eta_{5\%} + 0.06 \cdot \eta_{10\%} + 0.13 \cdot \eta_{20\%} + 0.10 \cdot \eta_{30\%} + 0.48 \cdot \eta_{50\%} + 0.20 \cdot \eta_{100\%} \tag{2}$$

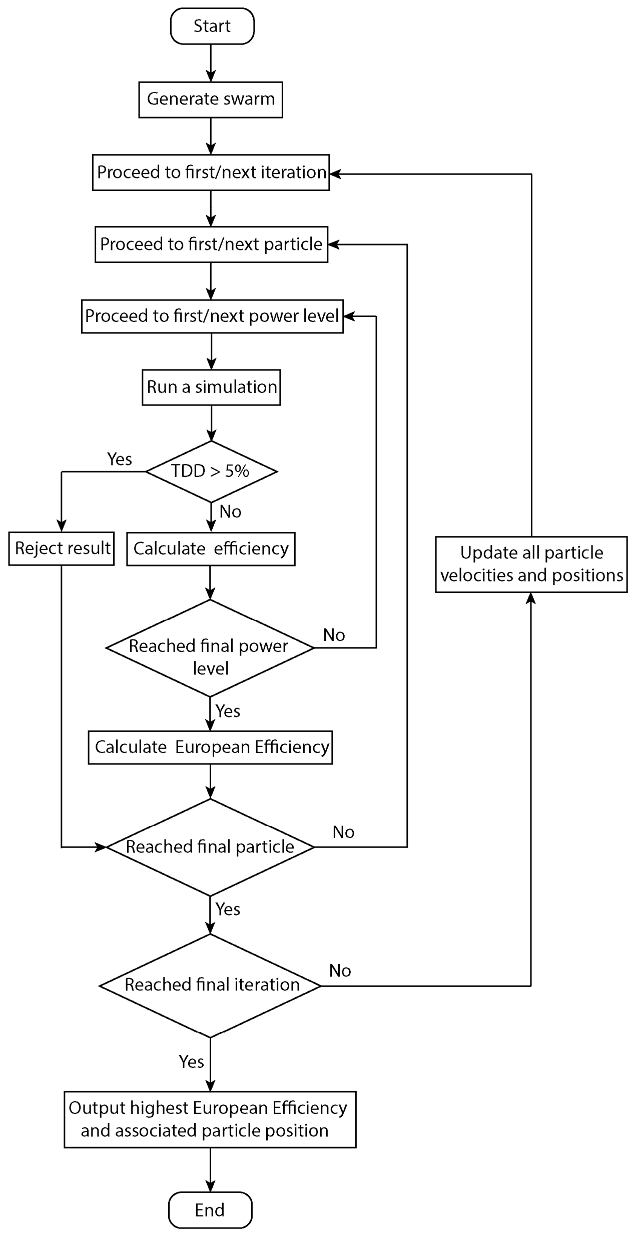

Fig. 2. Flowchart of the proposed design optimization algorithm.

In order to estimate the inverter losses and the TDD, the PV inverter and its controller are simulated in MATLAB-Simulink. The Simulink model is configured to adopt the parameter values of a given particle at its present position and run for a certain inverter power level. Hence, for every iteration of the PSO algorithm, the model is configured for all particles (one by one), and for each particle it is simulated at all power levels required for the calculation of η_{eu}. If while running the simulation for a given particle and power level, the current TDD exceeds 5%, the set of design values representing the present particle position is rejected (that is, it is not considered as potentially optimal solution of the optimization problem). If not, the inverter losses are estimated as explained in the following paragraph and retained to calculate the European efficiency for this particle. A flowchart of the proposed design optimization algorithm is presented in Fig. 2.

C. Estimation of PV inverter losses

The selected inverter semiconductors are power MOSFETs. The MOSFETs are simulated using Simscape Physical System (PS) blocks, together with their cooling system. This provides the capability to estimate their conduction and switching losses, as well as the resulting junction temperature. Conduction losses are estimated based on the MOSFET $R_{DS,on}$. Switching loss (E_{on}/E_{off}) data are provided to the Simulink MOSFET blocks using piecewise linear approximation of loss curves derived based on the MOSFET and the gate driver characteristics. All loss curves are provided for two (or more) different junction temperatures. The Simulink model of the PV inverter calculates the conduction and switching losses during the simulation and uses them to calculate the junction temperature of the semiconductors. The junction temperature is, in turn, used for interpolation between the provided loss curves. The MOSFET model selected for the simulations of the present study is the NTHL040N65S3HF by Onsemi, having an $R_{ds,on}$ of 40 / 72mΩ at a junction temperature of 25 / 125 ºC, respectively. Its switching losses (total for turn-on and turn-off) were estimated according to [24] to be 970μJ at 300V – 10A and are scaled in the Simulink model according to the instantaneous voltage – current values.

The copper losses of the inductors and the capacitor are calculated considering their Equivalent Series Resistances (ESRs), as

$$P_{L\_loss} = I_{L,RMS}{}^2 \cdot ESR_L \quad (3)$$

$$P_{C\_loss} = I_{C,RMS}{}^2 \cdot ESR_C \quad (4)$$

where ESR_L and ESR_C are varied proportionally with the value of L (and L_f) and C, respectively, and ESR_L = 44mΩ for L = 1mH and ESR_C =15mΩ for C = 3μF.

The inductor core losses are estimated based on the improved Generalized Steinmetz Equation (iGSE) method, proposed in [25]. This employs the Steinmetz's equation

$$\bar{P}_u = k \cdot f^a \cdot \hat{B}^b \quad (5)$$

where P_u stands for the time average power loss per unit volume (in W/cm³), f is the excitation (i.e. the switching) frequency, B is the peak magnetic flux density and k, a and b are the Steinmetz coefficients. The latter are determined by the material's *B-H* hysteresis curve and their values are listed in Table II.

TABLE II. INDUCTOR CORE LOSS PARAMETERS

Parameter	Value
Material	N87
k	5e-5 (W/cm³)
a	1.13
b	2.16

IV. RESULTS

In order to demonstrate the effectiveness of the proposed method, the topology of Fig. 1 was modelled as a 2kVA inverter with the abovementioned MOSFET and filter parameters. The PV array voltage at the Maximum Power Point (MPP) was approximately 250V, while the grid voltage/frequency were set to 230V/50Hz.

The proposed algorithm was then executed with two different sets (cases) of constraints: Case A – Considering only the boundary values of Table I, and Case B – Imposing an additional constraint to the overall size of the filter inductors, expressed in the form of (6), below:

$$4 \cdot L + L_f < 3\text{mH} \quad (6)$$

The coefficient before L is set to 4 because this inductor must be rated at about twice the current of inductor L_f, and thus for the same inductance it will be four times greater in size. The limit of 4mH is used as an example and corresponds to a given allowed total inductor volume.

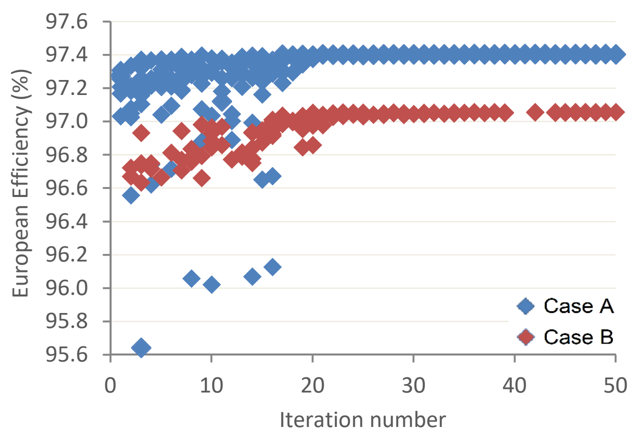

(a)

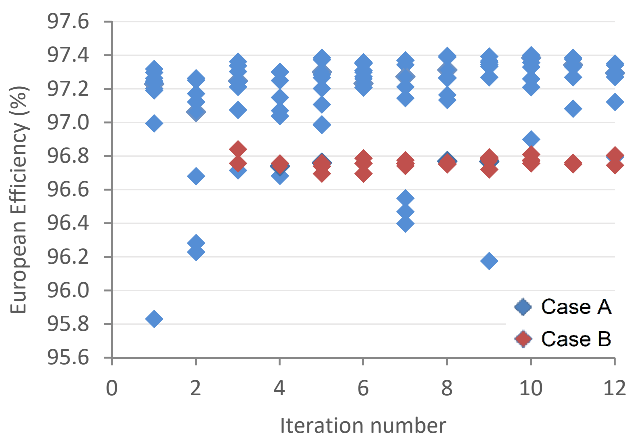

(b)

Fig. 3. Resulting European efficiency for all accepted particles per PSO algorithm iteration, for the two design cases, (a) without, and (b) with the application of a η_{eu} relative change stopping criterion.

Fig. 3(a) illustrates the derived European efficiency for both cases of constraints, for all accepted (i.e. with TDD < 5%) particles during the first 50 iterations of the PSO algorithm evolution. It can be observed that the algorithm generates particle positions that, on average, obtain consistently higher European efficiencies. It was noticed, however, that the maximum value of European efficiency was actually determined (by a single particle) in the first few iterations. Thus, a stopping criterion was introduced to the algorithm, according to which it terminated when the relative change in the highest value of European efficiency found after 10 successive iterations was less than 0.01%. By applying this criterion, the PSO algorithm for both design cases terminated after only 12 iterations, as shown in Fig. 3(b). The algorithm was still able to locate solutions that achieved near-optimal European efficiencies, but within significantly reduced execution times. To provide a time scale, the 50 / 12 iterations for each design case required approximately 33 / 8 hours on a PC with an Intel Core^{TM} i3-8100 CPU at 3.60 GHz and 8.00 GB RAM, running MATLAB-Simulink version R2020a.

The optimized values for the design parameters and the obtained European efficiencies for the two design cases are shown in Table III. The latter were calculated from the individual efficiencies achieved at each power level, shown in Fig. 4. The loss distribution among the considered components of the PV inverter is presented in Fig. 5. The capacitor losses were not included in this figure, because they are one order of magnitude lower than the inductor losses.

TABLE III. OPTIMIZED PARAMETERS AND EUROPEAN EFFICIENCY

Symbol	Case A	Case B	Unit
f_s	10000	14231	Hz
L	1.4935	0.5333	mH
L_f	0.2350	0.7197	mH
C	4.3719	5.0000	μF
η_{eu}	97.40	96.84	%

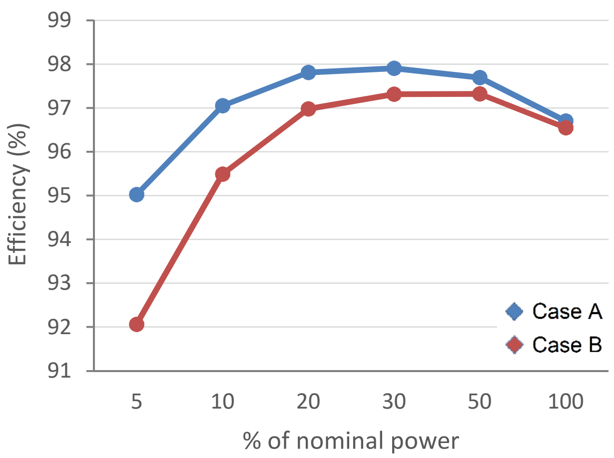

Fig. 4. Efficiency obtained at each power level specified in the formula for η_{eu}, for the two design cases.

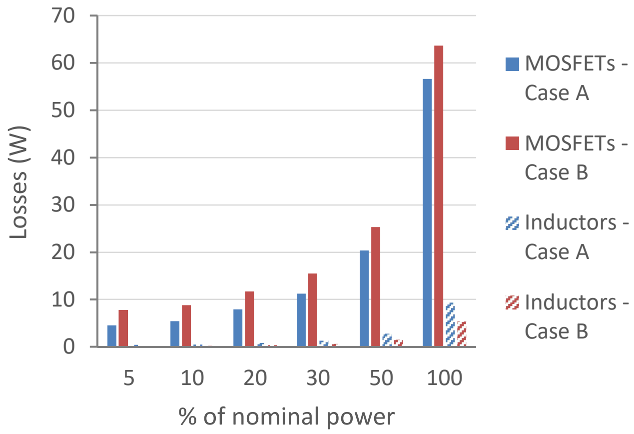

Fig. 5. MOSFET and inductor losses at each power level specified in the formula for η_{eu}, for the two design cases.

Moreover, it can be observed from Fig. 5 that the inductor losses are consistently lower that the respective MOSFET losses, by at least 5 times. This is the reason why in Case A, the proposed algorithm located the maximum European efficiency at the minimum allowed switching frequency and optimized the filter parameters based on the restriction on TDD. In Case B, on the other hand, the switching frequency was increased to allow for lower inductor values, so that the restriction on the total inductor volume is met.

V. CONCLUSION

This paper presented an inverter design optimization approach focusing on the key requirements for Aalborg-type transformerless PV inverters, of maximum European efficiency and permissible output current distortion. By means of complete system simulations, executed only a limited number of times with heuristically selected sets of design parameters, it was feasible to identify the optimal values for these parameters under two different example sets of constraints. The proposed method has the advantage that it can also be applied to unconventional converter topologies and/or modulation and control strategies, without requiring derivation of analytical expressions for semiconductor and passive component losses. Analytical approximations for estimating the values of power quality indices are not required, either, since these can also be calculated as part of the simulations. The method can be adapted to operate with different loss models and constraints, while it can be extended to multi-objective optimization by applying weighting factors to different objectives, or by employing multi-objective optimization algorithms.

ACKNOWLEDGMENT

This work was performed within the framework of the project "eSOLAR: Principle and control of high-efficiency Buck-Boost type Photovoltaic inverter" of the program "Bilateral and Multilateral Research & Technology Co-operation between Greece and China", funded by the Operational Program "Competitiveness, Entrepreneurship and Innovation 2014-2020" (co-funded by the European Regional Development Fund) and managed by the General Secretariat of Research and Technology, Ministry of Education, Research, and Religious Affairs under the project eSOLAR/T7ΔKI-00066. This support is gratefully acknowledged.

REFERENCES

[1] M. Delhommais, "Review of optimization methods for the design of power electronics systems," *22nd European Conference on Power Electronics and Applications (EPE'20 ECCE Europe)*, 2020, pp. 1-10.

[2] S. E. De León-Aldaco, H. Calleja and J. Aguayo Alquicira, "Metaheuristic Optimization Methods Applied to Power Converters: A Review," in *IEEE Transactions on Power Electronics*, vol. 30, no. 12, pp. 6791-6803, Dec. 2015.

[3] B. Cheong, P. Giangrande, X. Zhang, M. Galea, P. Zanchetta and P. Wheeler, "System-Level Motor Drive Modelling for Optimization-based Designs," *21st European Conference on Power Electronics and Applications (EPE '19 ECCE Europe)*, 2019, pp. 1-9.

[4] B. Cheong, P. Giangrande, X. Zhang, M. Galea, P. Zanchetta and P. Wheeler, "Fast and Accurate Multi-Physics Model for Optimization-based Design of VSBBC," *IECON 2019 - 45th Annual Conference of the IEEE Industrial Electronics Society*, 2019, pp. 1762-1767.

[5] Y. Chen, Z. Yuan and F. Luo, "A Model-Based Multi-Objective Optimization for High Efficiency and High Power Density Motor Drive Inverters for Aircraft Applications," *NAECON 2018 - IEEE National Aerospace and Electronics Conference*, 2018, pp. 36-42.

[6] I. Laird, X. Yuan, J. Scoltock and A. J. Forsyth, "A Design Optimization Tool for Maximizing the Power Density of 3-Phase DC–AC Converters Using Silicon Carbide (SiC) Devices," in *IEEE Transactions on Power Electronics*, vol. 33, no. 4, pp. 2913-2932, April 2018.

[7] G. Adinolfi, G. Graditi, P. Siano and A. Piccolo, "Multiobjective Optimal Design of Photovoltaic Synchronous Boost Converters Assessing Efficiency, Reliability, and Cost Savings," in *IEEE Transactions on Industrial Informatics*, vol. 11, no. 5, pp. 1038-1048, Oct. 2015.

[8] R. M. Burkart and J. W. Kolar, "Comparative η–ρ–σ Pareto Optimization of Si and SiC Multilevel Dual-Active-Bridge Topologies With Wide Input Voltage Range," in *IEEE Transactions on Power Electronics*, vol. 32, no. 7, pp. 5258-5270, July 2017.

[9] E. Kantar and A. M. Hava, "Optimal Design of Grid-Connected Voltage-Source Converters Considering Cost and Operating Factors," in *IEEE Transactions on Industrial Electronics*, vol. 63, no. 9, pp. 5336-5347, Sept. 2016.

[10] E. Koutroulis, Y. Yang and F. Blaabjerg, "Co-Design of the PV Array and DC/AC Inverter for Maximizing the Energy Production in Grid-Connected Applications," in *IEEE Transactions on Energy Conversion*, vol. 34, no. 1, pp. 509-519, March 2019.

[11] D-D Tran, S. Chakraborty,Y. Lan, M. Baghdadi and O. Hegazy, "NSGA-II-Based Codesign Optimization for Power Conversion and Controller Stages of Interleaved Boost Converters in Electric Vehicle Drivetrains," in *Energies*, vol. 13, no. 19, October 2020.

[12] IEEE Std. 1547-2003, "IEEE Standard for Interconnecting Distributed Resources with Electric Power Systems".

[13] IEEE. IEEE recommended practice and requirements for harmonic control in electric power systems. In IEEE Standards Association; IEEE Power and Energy Society: Piscataway, MJ, USA, 2014; p. 29.

[14] C. Gurrola-Corral, J. Segundo, M. Esparza and R. Cruz, "Optimal LCL-filter design method for grid-connected renewable energy sources," *International Journal of Electrical Power & Energy Systems*, vol. 120, 2020.

[15] H. Kragh, F. Blaabjerg and J. K. Pedersen, "An advanced tool for optimised design of power electronic circuits," *Conference Record of 1998 IEEE Industry Applications Conference. Thirty-Third IAS Annual Meeting*, 1998, pp. 991-998, vol. 2.

[16] K. Rigbers, S. Schroder, T. Durbaum, M. Wendt and R. W. De Doncker, "Integrated method for optimization of power electronic circuits," *IEEE 35th Annual Power Electronics Specialists Conference*, 2004, pp. 4473-4478, vol. 6.

[17] J. Zhang, H. S. Chung, A. W. Lo and T. Huang, "Extended Ant Colony Optimization Algorithm for Power Electronic Circuit Design," in *IEEE Transactions on Power Electronics*, vol. 24, no. 1, pp. 147-162, Jan. 2009.

[18] Z. Zhan and J. Zhang, "Differential evolution for power electronic circuit optimization," *2015 Conference on Technologies and Applications of Artificial Intelligence (TAAI)*, 2015, pp. 158-163.

[19] M. Mirjafari and R. S. Balog, "Survey of modelling techniques used in optimisation of power electronic components," in *IET Power Electronics*, vol. 7, no. 1, pp. 1192-1203, Oct. 2014.

[20] J. Zhang, Y. Shi, and Z. H. Zhan, "Power electronic circuits design: A particle swarm optimization approach," *7th International Conference on Simulated Evolution And Learning (SEAL)*, 2008, pp. 605–614.

[21] W. Wu, J. Ji, and F. Blaabjerg, "Aalborg inverter—A new type of "Buck in Buck, Boost in Boost" Grid-Tied inverter," in *IEEE Transactions on Power Electronics*, vol. 30, no. 9, pp. 4784–4793, Sept. 2015.

[22] G. I. Orfanoudakis, E. Koutroulis, G. Foteinopoulos and W. Wu, "Synchronous Reference Frame current control of Aalborg-type PV inverters," *23rd European Conference on Power Electronics and Applications (EPE'21 ECCE Europe)*, 2021, pp. 1-10.

[23] J. Kennedy and R. Eberhart, "Particle swarm optimization," *Proceedings of ICNN'95 - International Conference on Neural Networks*, 1995, pp. 1942-1948, vol. 4.

[24] D. Graovac, M. Purschel, and A. Kiep, "MOSFET Power Losses Calculation Using the Datasheet Parameters, " Infineon Application Note, pp. 1–23, 2006.

[25] K. Venkatachalam, C. R. Sullivan, T. Abdallah and H. Tacca, "Accurate prediction of ferrite core loss with nonsinusoidal waveforms using only Steinmetz parameters," *IEEE Workshop on Computers in Power Electronics, 2002*, pp. 36-41.